mechanistic interpretations. However, under conditions where the reaction is run in limiting cysteine relative to BrMDHT concentration, the SN2 mechanism would predict that the ratio of thymine produced relative to cysteine utilized could not exceed 0.50, a restriction not placed on the E2 Hal mechanism because the second mole of $R\text{-}S^-$ required for cystine formation is involved in the reaction with a sulfenyl bromide and not with an intermediate (III) directly involved in thymine formation. Furthermore, only the E2 Hal mechanism would generate cysteic acid via the reaction of the sulfenyl bromide with $H_2O$. Consequently, under conditions of limiting cysteine concentration, the presence of cysteic acid as a product coupled with thymine to initial cysteine ratios consistently greater than 0.50 demonstrates that the E2 Hal mechanism is at least partially responsible for the debromination of BrMDHT. These results do not, however, eliminate the SN2 mechanism as being important in the overall dehalogenation of the halouracils by cysteine, as the E2 Hal mechanism alone cannot account for the 5-cysteinyluracil found as products in the work of Wataya et al.[9] Consequently, both mechanisms must be considered as feasible candidates for the thiol-catalyzed dehalogenation of the halogenated pyrimidines; however, their relative contribution likely varies depending upon reactant concentrations, the nature of the halogen atom, and substituents on the pyrimidine ring system.

**Acknowledgments.** This work was supported by U.S. Public Health Service Grant No. CA-12971 from the National Institute of Cancer. We wish to thank Dr. Ian Pitman, Department of Pharmaceutical Chemistry, University of Kansas, for generously giving us an authentic sample of 5-bromo-6-methoxy-5,6-dihydrothymine and for communicating his results on the $SO_3^{2-}$ promoted dehalogenation of the 5-halodihydrouracils prior to publication.

## References and Notes

(1) E. G. Sander and C. A. Deyrup, *Arch. Biochem. Biophys.*, **150**, 600 (1972).
(2) F. A. Sedor and E. G. Sander, *Arch. Biochem. Biophys.*, **164**, 632 (1974).
(3) D. G. Jacobson, F. A. Sedor, and E. G. Sander, *Bioorg. Chem.*, **4**, 72 (1975).
(4) F. A. Sedor, D. G. Jacobson, and E. G. Sander, *J. Am. Chem. Soc.*, **97**, 5572 (1975).
(5) G. S. Rork and I. H. Pitman, *J. Am. Chem. Soc.*, **97**, 5566 (1975).
(6) G. S. Rork and I. H. Pitman, *J. Am. Chem. Soc.*, **97**, 5559 (1975).
(7) J. L. Fourrey, *Bull. Soc. Chim. Fr.*, 4580 (1972).
(8) F. A. Sedor and E. G. Sander, *Biochem. Biophys. Res. Commun.*, **50**, 328 (1973).
(9) Y. Wataya, K. Negishi, and H. Hayatsu, *Biochemistry*, **12**, 3992 (1973).
(10) F. A. Sedor, D. G. Jacobson, and E. G. Sander, *Bioorg. Chem.*, **3**, 154 (1974).
(11) R. Duschinsky, T. Gabriel, W. Tautz, A. Nussbaum, M. Hoffer, E. Grunberg, J. Burchenal, and J. J. Fox, *J. Med. Chem.*, **10**, 47 (1967).
(12) G. L. Ellman, *Arch. Biochem. Biophys.*, **82**, 70 (1959).
(13) J. B. Lombardini, P. Turini, D. R. Biggs, and T. P. Singer, *Physiol. Chem. Phys.*, **1**, 1 (1969).
(14) E. G. Sander, *J. Am. Chem. Soc.*, **91**, 3629 (1969).
(15) P. C. Jocelyn, "Biochemistry of the SH Group", Academic Press, London, 1972, pp 103–104.
(16) E. C. F. Ko and A. J. Parker, *J. Am. Chem. Soc.*, **90**, 6447 (1968).

# Monosodium Urate Monohydrate, the Gout Culprit

**Neil S. Mandel* and Gretchen S. Mandel**

*Contribution No. 5176 from the Norman W. Church Laboratory of Chemical Biology, California Institute of Technology, Pasadena, California 91125.*
*Received September 22, 1975*

**Abstract:** Crystals of monosodium urate monohydrate, $NaC_5H_3N_4O_3 \cdot H_2O$, are responsible for the inflammatory disease acute gouty arthritis. The crystals are triclinic needles, space group $P\bar{1}$, with $a = 10.888$ (5) Å, $b = 9.534$ (3) Å, $c = 3.567$ (1) Å, $\alpha = 95.06$ (3)°, $\beta = 99.47$ (5)°, $\gamma = 97.17$ (3)°, and $Z = 2$. The structure was solved by Patterson techniques and refined to a final $R$ index of 0.094 for 579 observed reflections. The urate anions are hydrogen bonded together about three centers of symmetry to form sheets nearly parallel to (011). Sodium ion coordination leads to a rippling of the sheets by inducing a 7.7° tilt of the purine rings from the (011) plane and may also be partially responsible for the very intimate (3.28 Å) stacking of the urate ions. The crystal faces which interact with the lysosomal membrane during a gouty attack contain stacks of edge-on urate anions separated by stacks of sodium ions and water molecules.

The presence of crystalline monosodium urate monohydrate in the human body is prerequisite to the disease acute gouty arthritis. Electron microscopy has clearly indicated the encapsulation of the inflammatory salt crystals by white blood cells, polymorphonuclear leukocytes (PMN's), during gouty attacks.[1] The physiological function of a PMN is to phagocytize foreign materials and digest them using the digestive enzymes contained within one of its organelles, the lysosome. When crystals of monosodium urate monohydrate are phagocytized, the normal digestive process is initiated with enzymatic degradation of the protein coat adhering to the crystal. Very soon after this initial digestion, the lysosomal membrane, which separates the digestive process from the cytoplasm, lyses. The result is uncontained enzymatic activity within the entire leukocyte, leading to the rupture of the plasma membrane, and the release of the lysosomal enzymes into the serum surrounding the leukocyte. It is the release of these enzymes into the serum that precipitates the pain and inflammation associated with acute gouty arthritis.

The currently accepted mechanism for this crystal-induced membranolysis[2,3] invokes hydrogen-bond formation between donors on the crystal surface and the oxygen atoms of the phosphate head groups of the phospholipid membrane. The long-range cooperative effect of these hydrogen bonds is to bind the membrane so tightly that it becomes more rigid and tears open at the crystal edges as the membrane undulates. The single-crystal structure of monosodium urate monohydrate is of utmost importance in the verification of this mechanism or consequently in the postulation of any alternative mechanism.

## Experimental Section

The colorless needles were grown by adding uric acid (Nutri-

Table I. Crystal Data for $NaC_5H_3N_4O_3 \cdot H_2O$

| | |
|---|---|
| $a$ = 10.888 (5) Å | Space group $P\bar{1}$ |
| $b$ = 9.534 (3) Å | $Z$ = 2 |
| $c$ = 3.567 (1) Å | $D_m$ = 1.90 g cm$^{-3}$ |
| $\alpha$ = 95.06 (3)° | $D_c$ = 1.92 g cm$^{-3}$ |
| $\beta$ = 99.47 (5)° | $\lambda$(Cu K$\alpha$) = 1.5418 Å |
| $\gamma$ = 97.17 (3)° | $\mu$ = 19.6 cm$^{-1}$ |

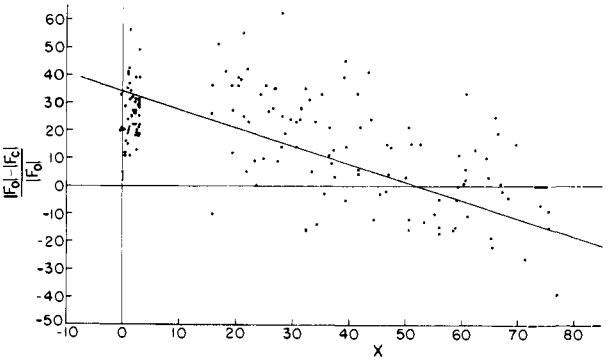


**Figure 1.** Plot of $(|F_o| - |F_c|)/|F_o|$ vs. $\chi$.

tional Biochemical Corp., Cleveland, Ohio) to boiling 0.025 M borax buffer until reaching saturation (final pH 9.29). The hot solution was poured into test tubes which were then buried in sand at 95 °C. The temperature of the sand was lowered over a period of 3 weeks. The vast majority of crystals formed were very small, multitwinned needles. One crystal, 0.03 × 0.06 × 0.40 mm, was suitable for data collection and was mounted along its needle ($c$) axis. The synthetic crystals were shown to be identical with the in vivo inflammatory material by comparison of powder diffraction lines.[4]

Approximate unit-cell dimensions were obtained from preliminary zero- and first-level Weissenberg photographs. More accurate lattice constants were obtained from a least-squares fit of $\sin^2\theta$ values for 24 singly indexed powder-diffraction lines recorded in a Guinier-Hägg powder camera equipped with a focusing quartz monochromator and Cu K$\alpha$ radiation. Crystal data are given in Table I. The density was measured by flotation in a methanol-ethylene bromide solution.

The crystal had very broad mosaic character as evidenced by the diffuseness of all reflections observed on the preliminary Weissenberg photographs. The width of these reflections along the spindle axis ranged from 6 to 8°, whereas the $2\theta$ basewidth only spanned 1-2°. The intensity distribution along the long axis of the photographic diffraction spot was essentially a continuum, with one end somewhat more intense than the other. Diffractometer scans in $\phi$ and $2\theta$ were consistent with the photographic observations and, in addition, $\chi$ scans indicated two equal maxima approximately 0.5° apart. The half-width in $\phi$ was also noted to broaden with increasing values of $\chi$.

Table III. Coordinates (×10$^3$) for the Hydrogen Atoms[a]

| | $x$ | $y$ | $z$ |
|---|---|---|---|
| H(1) | 90 | −20 | −61 |
| H(7) | 530 | 105 | −210 |
| H(9) | 377 | 460 | −408 |
| H(10) | 90 | 670 | −50 |
| H(10') | 160 | 500 | −240 |

[a] The isotropic temperature factors for all hydrogen atoms were set at 3.50 Å$^2$.

Intensity data were collected at room temperature on a Datex-automated General Electric quarter-circle diffractometer equipped with Ni-filtered Cu K$\alpha$ radiation using the $\theta$-$2\theta$ scan mode, a scan speed of 0.5°/min, scan widths varying linearly from 2.0° at $2\theta$ = 5.0° to 3.0° at $2\theta$ = 150.0°, and 30-s background counts. The three standard reflections monitored throughout the data collection showed no unusual fluctuations or decay with time. A total of 1501 unique reflections was collected; 579 reflections had $I > 3\sigma(I)$.[5] Observational variances, $\sigma^2(I)$, included counting statistics plus an additional empirical term $(0.02S)^2$, where $S$ is the scan count. The intensities and their variances were corrected for Lorentz and polarization effects but not for absorption ($\mu$ = 19.6 cm$^{-1}$).

**Structure Determination and Refinement.** A Howells, Phillips, and Rogers[6] plot of intensities indicated a centric structure and therefore the centrosymmetric space group $P\bar{1}$ was assumed. A three-dimensional sharpened Patterson map indicated the positions of the Na atoms and the two urate-anion fragments hydrogen bonded across a center of symmetry. Subsequent difference-Fourier syntheses yielded the entire structure.

The urate anion was refined initially as a rigid group using the program UCIGLS[7] and later as individual atoms using the CRYM least-squares program. The quantity minimized in the full-matrix least-squares calculation was $\Sigma w(F_o^2 - F_c^2)^2$ with weights $w$ equal to $\sigma^{-2}(F_o^2)$. Atomic form factors for $Na^+$, O, N, and C were taken from the International Tables,[8] and those for H from Stewart et al.[9] The structure converged initially at an $R$ index, $\Sigma||F_o| - |F_c||/\Sigma|F_o|$, of 0.119 for the 579 reflections with $I > 3\sigma(I)$. At this stage, an analysis of the agreement between $F_o$ and $F_c$ indicated a systematic variation with the diffraction angle $\chi$, undoubtedly due to the increasing $\phi$ basewidth with increasing $\chi$. A plot of $(|F_o| - |F_c|)/|F_o|$ vs. $\chi$ (Figure 1) yielded an empirical scale factor used to correct for this aberration. This correction lowered the $R$ index to 0.094 and gave a goodness of fit, $[\Sigma w(F_o^2 - F_c^2)^2/n - p]^{1/2}$, of 4.40 for $p$ = 99 parameters and $n$ = 579 observations. Final atomic parameters are given in Table II. The anisotropic temperature parameters probably do not represent reality due to the approximate nature of the correction for the $\phi$-$\chi$ coupling. Certainly this empirical correction has not accounted for all of the systematic errors present in the data set.

The three hydrogen atoms of the urate anion were placed 0.95 Å from the corresponding nitrogen atoms. Positions for the two water-hydrogen atoms were also calculated; H(10') was positioned

Table II. Coordinates and Anisotropic Temperature Factors Coordinates (×10$^4$) and $U_{ij}$ Values (×10$^3$)[a]

| | $x$ | $y$ | $z$ | $U_{11}$ | $U_{22}$ | $U_{33}$ | $U_{12}$ | $U_{13}$ | $U_{23}$ |
|---|---|---|---|---|---|---|---|---|---|
| N(1) | 1473 (11) | 574 (12) | −1100 (36) | 43 (8) | 42 (8) | 46 (10) | −7 (7) | 16 (7) | 12 (6) |
| C(2) | 991 (15) | 1813 (16) | −1712 (42) | 47 (11) | 50 (10) | 28 (11) | 5 (9) | 2 (8) | 11 (8) |
| O(2) | −167 (9) | 1845 (9) | −1512 (32) | 43 (8) | 48 (7) | 74 (9) | 10 (6) | 19 (6) | 26 (6) |
| N(3) | 1728 (11) | 2973 (11) | −2556 (34) | 49 (8) | 34 (7) | 45 (10) | −11 (6) | 13 (7) | 11 (6) |
| C(4) | 2910 (14) | 2696 (14) | −2635 (41) | 45 (10) | 22 (7) | 35 (11) | 1 (7) | 15 (8) | 7 (7) |
| C(5) | 3453 (13) | 1473 (13) | −1932 (41) | 35 (9) | 25 (8) | 42 (11) | −7 (7) | 0 (8) | 11 (7) |
| C(6) | 2718 (14) | 312 (14) | −1080 (40) | 61 (11) | 27 (8) | 33 (11) | 11 (8) | 12 (8) | 7 (7) |
| O(6) | 3007 (8) | −895 (9) | −566 (30) | 61 (8) | 30 (6) | 73 (9) | 14 (5) | 11 (6) | 21 (6) |
| N(7) | 4715 (10) | 1714 (10) | −2389 (34) | 42 (8) | 22 (6) | 53 (10) | 9 (6) | 13 (7) | 13 (6) |
| C(8) | 4959 (13) | 3080 (13) | −3342 (40) | 33 (9) | 33 (8) | 35 (10) | −3 (7) | 3 (8) | 11 (7) |
| O(8) | 5993 (8) | 3641 (8) | −3906 (28) | 36 (6) | 29 (5) | 52 (8) | 2 (5) | 10 (5) | 21 (5) |
| N(9) | 3863 (10) | 3664 (10) | −3481 (32) | 31 (7) | 24 (6) | 50 (9) | 2 (5) | 12 (6) | 15 (6) |
| Na | 7872 (5) | 2645 (5) | −3611 (17) | 47 (4) | 36 (3) | 52 (5) | 9 (3) | 10 (3) | 18 (3) |
| O(10) | 1239 (8) | 5831 (8) | −2270 (29) | 57 (7) | 36 (6) | 69 (9) | 22 (5) | 15 (6) | 10 (6) |

[a] Standard deviations are given in parentheses. The anisotropic temperature coefficients are of the form $\exp(-2\pi^2)(h^2a^{*2}U_{11} \ldots + 2klb^*c^*U_{23})$.

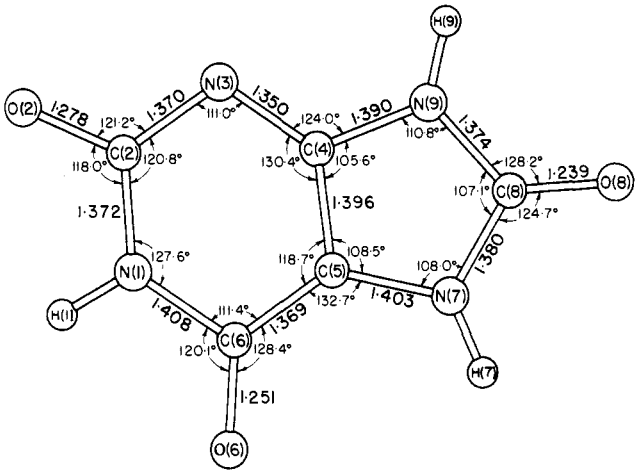


**Figure 2.** Bond distances and angles of the urate anion. The estimated standard deviations are 0.015 Å and 1.0°.

along the presumed hydrogen bond between O(10) and N(3), and H(10) was placed 109° from H(10′) and equidistant between the two sodium ions coordinated to O(10). Despite an O(10)····O(2) distance of 2.95 Å, we do not think that H(10) is hydrogen bonded to O(2). This arrangement would be contrary to the observation[10] that hydrogen atoms are only rarely located along the edges of cation coordination polyhedra. The repulsive interaction between a hydrogen atom and a metal cation is presumably greater than the attractive force of a hydrogen bond. It is interesting to note that the assumed position of H(10) is approximately equidistant between two neighbors O(2) and O(10), at 2.54 and 2.65 Å, respectively. Hydrogen atom coordinates are given in Table III.

## Discussion

Bond distances and angles in the urate anion are shown in Figure 2. The tautomeric form of the urate anion corresponds to the deprotonation of N(3). A comparison (Table IV) of the bond distances of the urate anion in the present structure with those of uric acid,[11] sodium xanthine,[12] and guanine monohydrate[13] indicates that the negative charge formally resident on N(3) has been delocalized over the entire six-membered ring. The lengthening of the C(2)-O(2) and C(6)-O(6) bonds implies that O(2) and O(6) aid in the negative charge delocalization and that they utilize the negative charge in strengthening their sodium ion coordination. This charge delocalization is consistent with the very short

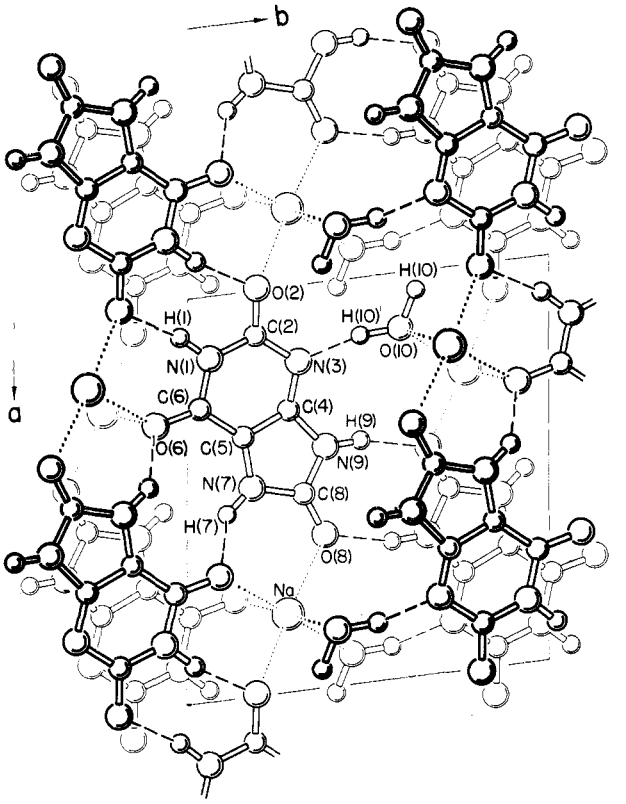


**Figure 3.** A view down $c^*$, indicating sodium ion coordination, hydrogen bonding, and extensive base stacking. The angle between the needle axis $c$ and $c^*$ is 11.4°.

interplanar spacing of 3.28 Å between the highly overlapped, negatively charged bases. Unfortunately, the high standard deviations in this structure prevent a more detailed analysis of the resonance form of the urate anion.

A view down $c^*$ is shown in Figure 3. The angle between the needle axis $c$ and $c^*$ is 11.4°. Each urate anion is hydrogen bonded across three centers of symmetry forming sheets parallel to (011). The sheets are held together by stacking interactions and by interlayer coordination to the sodium ions. The water molecule is held in the structure by coordination to two sodium ions and by one hydrogen bond to the purine ring.

Table IV. A comparison of Purine Bond Distances (Å)[a]

| | 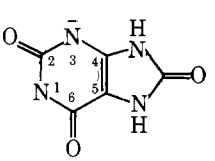 Na urate (0.015 Å) | 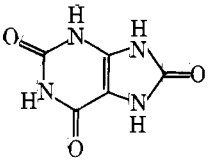 Uric acid[b] (0.005 Å) | 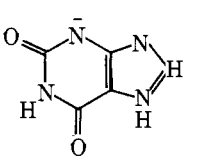 Na xanthine[c] (0.012 Å) | 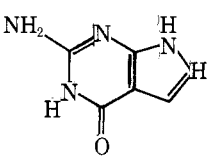 Guanine[d] (0.012 Å) |
|---|---|---|---|---|
| N(1)–C(2) | 1.372 | 1.367 | 1.38 | 1.371 |
| C(2)–N(3) | 1.370 | 1.382 | 1.33 | 1.315 |
| N(3)–C(4) | 1.350 | 1.356 | 1.36 | 1.364 |
| C(4)–C(5) | 1.396 | 1.360 | 1.37 | 1.392 |
| C(5)–C(6) | 1.369 | 1.411 | 1.41 | 1.405 |
| C(6)–N(1) | 1.408 | 1.397 | 1.39 | 1.398 |
| C(5)–N(7) | 1.403 | 1.387 | 1.41 | 1.405 |
| N(7)–C(8) | 1.380 | 1.359 | 1.30 | 1.319 |
| C(8)–N(9) | 1.374 | 1.376 | 1.37 | 1.369 |
| N(9)–C(4) | 1.390 | 1.360 | 1.36 | 1.364 |
| C(2)–O(2) | 1.278 | 1.223 | 1.26 | |
| C(6)–O(6) | 1.251 | 1.233 | 1.26 | 1.239 |
| C(8)–O(8) | 1.239 | 1.241 | 1.26 | |

[a] Values in parentheses are approximate estimated standard deviations. [b] See ref 11. [c] See ref 12. [d] See ref 13.

Table V. Sodium–Oxygen Distances (Å) and Oxygen–Sodium–Oxygen Angles (deg) in the Sodium Ion Coordination[a]

| Atom | Distance | Oxygen atoms of the O–Na–O angles | | Angles |
|---|---|---|---|---|
| O(2) [100, 1] | 2.384 | O(2) [100, 1] | O(6) [10$\bar{1}$, 2] | 101.1 |
| O(6) [10$\bar{1}$, 2] | 2.520 | | O(6) [100, 2] | 85.2 |
| O(6) [100, 2] | 2.535 | | O(8) [000, 1] | 164.4 |
| O(8) [000, 1] | 2.351 | | O(10) [11$\bar{1}$, 2] | 92.3 |
| O(10) [11$\bar{1}$, 2] | 2.387 | | O(10) [110, 2] | 75.8 |
| O(10) [110, 2] | 2.427 | O(6) [10$\bar{1}$, 2] | O(6) [100, 2] | 89.8 |
| | | | O(8) [000, 1] | 92.7 |
| | | | O(10) [11$\bar{1}$, 2] | 87.8 |
| | | | O(10) [110, 2] | 175.4 |
| | | O(6) [100, 2] | O(8) [000, 1] | 87.6 |
| | | | O(10) [11$\bar{1}$, 2] | 176.2 |
| | | | O(10) [110, 2] | 86.6 |
| | | O(8) [000, 1] | O(10) [11$\bar{1}$, 2] | 95.4 |
| | | | O(10) [110, 2] | 90.1 |
| | | O(10) [11$\bar{1}$, 2] | O(10) [110, 2] | 95.6 |

[a] The values in brackets are unit cell translations and equivalent position numbers (where equivalent position 1 is $x,y,z$ and 2 is $\bar{x},\bar{y},\bar{z}$). Esd's are of the order of 0.009 Å and 0.3°.

Table VI. Details of the Hydrogen Bonds, D–H. . .A[a]

| Atom | | | Distance, Å | | Angle, deg |
|---|---|---|---|---|---|
| D | H | A | D. . .A | H. . .A | D–H. . .A |
| N(1) | H(1) | O(2) | 2.864 | 1.94 | 163 |
| N(7) | H(7) | O(6) | 2.764 | 1.96 | 141 |
| N(9) | H(9) | O(8) | 2.805 | 1.89 | 162 |
| O(10) | H(10′) | N(3) | 2.837 | 1.91 | 179 |
| O(10)[b] | H(10) | O(2) | 2.954 | 2.54 | 108 |
| O(10)[b] | H(10) | O(10) | 3.201 | 2.65 | 120 |

[a] Hydrogen atom positions were calculated as discussed in the text. [b] Not considered to be a hydrogen bond.

Table VII. Deviation (Å) from the Plane of the Purine Ring[a]

| Atom | Deviation | Atom | Deviation |
|---|---|---|---|
| N(1) | −0.014 | H(1) | −0.046 |
| C(2) | 0.001 | H(7) | 0.016 |
| O(2) | −0.007 | H(9) | −0.030 |
| N(3) | 0.006 | Na | 0.015 |
| C(4) | 0.006 | O(10)[b] | 0.639 |
| C(5) | 0.029 | O(2)[c] | 0.269 |
| C(6) | 0.026 | O(6)[d] | 0.975 |
| O(6) | −0.028 | O(8)[e] | −0.320 |
| N(7) | 0.014 | | |
| C(8) | −0.009 | | |
| O(8) | −0.011 | | |
| N(9) | −0.013 | | |

[a] Least-squares plane passed through O(2), O(6), O(8), and the nine ring atoms N(1)–N(9), all weighted equally. [b] Donor in hydrogen bond to N(3). [c] Acceptor in hydrogen bond from N(1). [d] Acceptor in hydrogen bond from N(7). [e] Acceptor in hydrogen bond from N(9).

The details of the sodium coordination are given in Table V and are emphasized in Figure 3. The sodium ion coordination is approximately octahedral with an average sodium-oxygen distance of 2.44 (8) Å and a range of nearest-neighbor angles between 76 and 101°.

Details of the hydrogen bonding scheme are given in Table VI and the planarity of the molecule is described in Table VII. The urate anion twists 7.7° out of the (011) plane on forming hydrogen bonds about three centers of symmetry. This twist is presumably required for the urate anions to form these three sets of hydrogen bonds while at the same time maintaining octahedral geometry about the Na ion. O(6) seems to be most affected by the competition between sodium coordination and hydrogen-bond formation. The two Na-O(6) distances are the largest in the Na coordination polyhedra and, further, the N(7)-O(6) distance of 2.76 Å is among the shorter N-O hydrogen-bonded contacts reported for purines.[14] The result of this competition is the displacement of the acceptor atom O(6) 0.462 Å from the (011) plane and 0.975 Å from the plane of the purine ring containing the donor atom N(7).

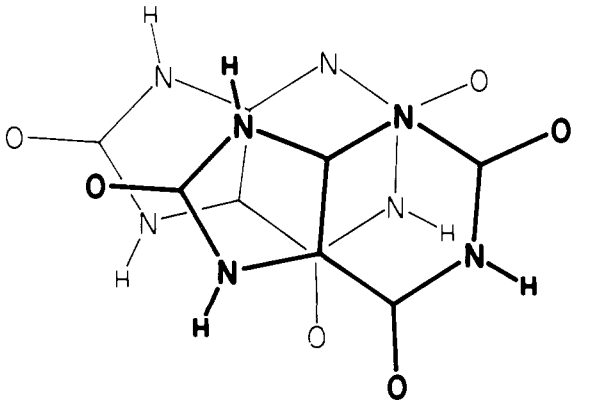

Figure 4. The base stacking of the urate anion, $d$ = 3.28 Å.

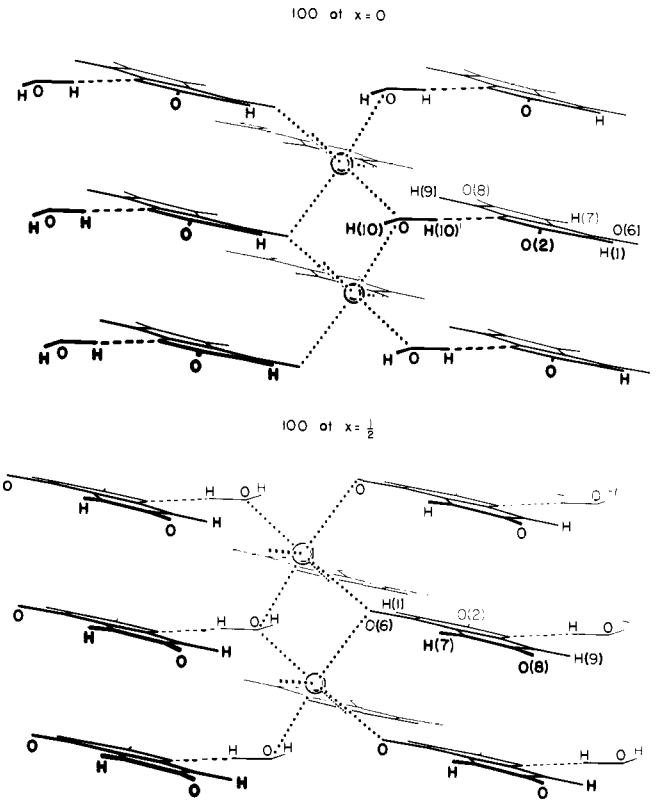


Figure 5. Views onto the (100) face.

The purine rings are related by lattice translations and therefore stack with the imidazole rings of adjacent bases pointing in exactly the same direction (Figure 4). With the extensive overlap caused by this type of stacking, it is surprising that the repulsions of the negative charges formally resident on urate anions do not increase the interplanar spacing, 3.28 Å, over that observed for neutral purines.[15] The charge delocalization by the sodium ion must be, at least in part, responsible for this effect.

The prominent crystal faces are of the form [100] and [010]. In vivo crystals of monosodium urate monohydrate always exhibit this same needle morphology. Since the faces along the needle axis constitute almost all the surface area,

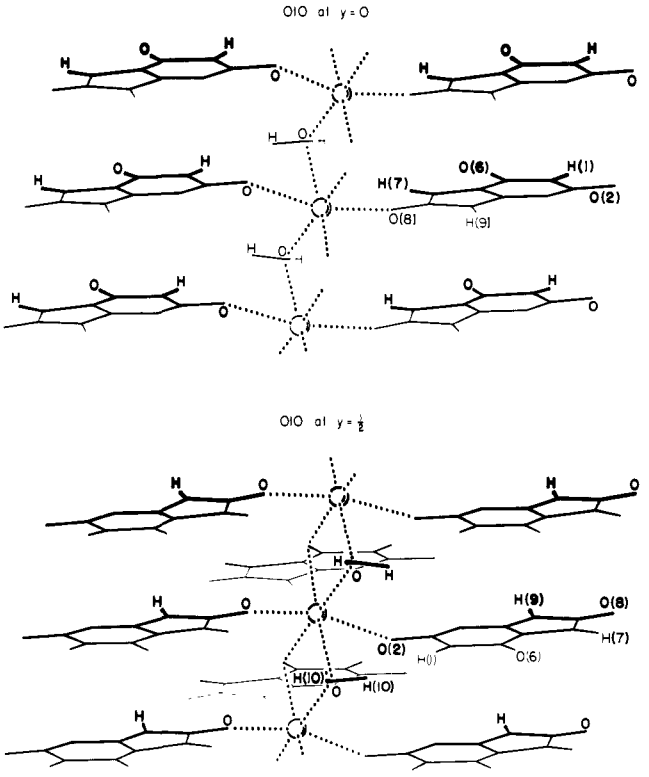


**Figure 6.** Views onto the (010) face.

any long-range molecular interaction with the membrane must involve these faces. Inspection of Figure 3 shows that there are two possible surfaces parallel to (100) at $x = 0$ and $x = \frac{1}{2}$ (Figure 5). To visualize these surfaces, the reader should imagine the atoms which are exposed by breaking the nonbonded contacts about $x = 0$ and about $x = \frac{1}{2}$. About $x = 0$ the exposed surface groups available for complexing with the lysosomal membrane are the unfilled coordination sites on the sodium cations, the slightly negative oxygen atoms O(2), and the hydrogen atoms H(1) of the urate anions and H(10) of the water molecules. For the surface at $x = \frac{1}{2}$, the exposed active groups are again the sodium ion, oxygen atoms O(6) and O(8), and the hydrogen atoms of urate anions H(7) and H(9). Similarly, the two possible surfaces parallel to (010) at $y = 0$ and $\frac{1}{2}$ are shown in Figure 6. About $y = 0$ the exposed surface contains two unfilled sites for each Na ion, the oxygen atoms O(2) and O(6), and hydrogen atoms H(1) and H(7) of the urate anion. The surface at $y = \frac{1}{2}$ contains only O(8) and H(9) of the urate anions and H(10′) of the water molecules.

We note that all of the exposed crystal surfaces contain hydrogen atoms which could be used in a hydrogen-bonding interaction with the membrane and, further, that these surfaces are also rich in charged oxygen atoms and sodium ions. In the proposed hydrogen-bonding mechanism, the acceptor atoms were thought to be the phospholipid phosphate oxygen atoms. However, the current model[16] for biological membranes puts these oxygen atoms beneath a layer of head groups and, hence, makes them unavailable for hydrogen bonding. In addition, compositional studies on the lysosomal membrane indicate that approximately 74% of the head groups are positively charged—choline, 56%, and ethanolamine, 18%.[17] Therefore, it is more likely that in any long-range hydrogen bonding interactions, the crystals would contain the acceptor rather than donor atoms. Alternatively, an electrostatic interaction between the oxygen atoms of the urate anions and the positively charged phospholipid head groups might play the crucial role in the binding of the lysosomal membrane.

**Acknowledgment.** We thank Dr. R. E. Marsh for his stimulating discussions during the structure solution and the preparation of this manuscript. Support was derived in part from the Arthritis and Metabolic Diseases Institute of the National Institutes of Health Fellowship Grant No. 1 F22 AM00988.

**Supplementary Material Available:** intensity data, 3 pages. Ordering information is given on any current masthead page.

## References and Notes

(1) H. R. Schumacher and P. Phelps, *Arthritis Rheum.*, **14**, 513–526 (1971).
(2) W. R. Wallingford and D. J. McCarty, *J. Exp. Med.*, **133**, 100–112 (1971).
(3) G. Weissman and G. A. Rita, *Nature (London), New Biol*, **240**, 167–172 (1972).
(4) R. Howells, E. D. Eanes, and J. E. Seegmiller, *Arthritis Rheum.*, **6**, 97–103 (1963).
(5) See paragraph at end of paper regarding supplementary material.
(6) E. R. Howells, D. C. Phillips, and D. Rogers, *Acta Crystallogr.*, **3**, 210–214 (1950).
(7) R. J. Doedens, "International Summer School of Crystallographic Computing, Carleton University 1969", Munksgaard, Copenhagen, 1970, pp 198–200.
(8) "International Tables for X-Ray Crystallography", Vol. III, Kynoch Press, Birmingham, 1962, pp 202–203.
(9) R. F. Stewart, G. R. Davidson, and W. T. Simpson, *J. Chem. Phys.*, **42**, 3175–3187 (1965).
(10) W. H. Baur, *Acta Crystallogr., Sect. B*, **28**, 1456–1465 (1972); W. H. Baur, *ibid.*, **29**, 139–140 (1973).
(11) H. Ringertz, *Acta Crystallogr.*, **20**, 397–403 (1966).
(12) H. Mizuno, T. Fujiwara, and K. Tomita, *Bull. Chem. Soc. Jpn.*, **42**, 3099–3105 (1969).
(13) U. Thewalt, C. E. Bugg, and R. E. Marsh, *Acta Crystallogr., Sect. B*, **27**, 2358–2363 (1971).
(14) D. Voet and A. Rich, *Prog. Nucleic Acid Res. Mol. Biol.*, **10**, 183–265 (1970).
(15) C. E. Bugg, "Proceedings, Fourth Jerusalem Symposium on the Purines: Theory and Experiment", Academic Press, New York, N.Y., 1971, pp 178–204.
(16) S. J. Singer and G. L. Nicolson, *Science*, **175**, 720–731 (1972).
(17) R. Henning and H. Heidrich, *Biochim. Biophys. Acta*, **345**, 326–335 (1974).